Biochimica et Biophysica Acta, 1057 (1991) 239–257
© 1991 Elsevier Science Publishers B.V. 0005-2728/91/$03.50
ADONIS 0005272891000988

BBABIO 43360

I. Langmuir-Blodgett monolayer films of bacterial photosynthetic membranes and isolated reaction centers: preparation, spectrophotometric and electrochemical characterization

Guillermo Alegria and P. Leslie Dutton

Department of Biochemistry and Biophysics, University of Pennsylvania, Philadelphia, PA (U.S.A.)

(Received 19 November 1990)

Key words: Langmuir-Blodgett film; Energy transduction; Bacterial reaction center; Photosynthetic bacterium

The Langmuir-Blodgett (LB) film technique has been successfully applied to the construction of stable and photo-active films of chromatophore membranes and isolated reaction centers from two species of photosynthetic bacteria, *Rhodobacter sphaeroides* and *Rhodopseudomonas viridis*. LB films of these preparations were characterized at the air/water interface through compression isotherms and film stabilities. Films deposited on glass slides were analyzed by spectrophotometric and redox potentiometric techniques. The results obtained indicate that the in vivo properties of the photosynthetic apparatus in the deposited films are essentially unchanged. Furthermore, the pigments and redox cofactors in the films are highly oriented and offer a unique opportunity for structural and functional studies of the kind described in the accompanying paper (Biochim. Biophys. Acta 1057 (1991) 258–272).

I. Introduction

Bacterial photosynthetic energy transduction is initiated in the reaction center protein (RC) by photoexcitation of a bacteriochlorophyll dimer, designated $BChl_2$. Electron donation from the excited dimer $BChl_2^*$ through a series of steps to the primary quinone acceptor, Q_A, generates a stable charge separated state $BChl_2^+Q_A^-$. Fig. 1 summarizes the energetics and kinetics of the charge separation reactions leading to the formation of $BChl_2^+Q_A^-$ and the routes for charge recombination in the isolated RC protein of *Rb. sphaeroides*. In the native membrane a *c*-type cytochrome reacts with the RC at the periplasmic side and serves to re-reduce the $BChl_2^+$; this helps prevent wasteful charge recombination and also prepares the RC for another photon. In some species like *Rhodobacter sphaeroides*, the cytochrome *c* is a soluble protein that binds and interacts with the RC on a mainly electrostatic basis, displaying complex electron transfer kinetics in the microsecond time scale (see Ref. 1). In other species like *Rhodopseudomonas viridis* and *Chromatium vinosum*, the cytochrome *c* polypeptide is hydrophobically complexed to the RC and contains four hemes, all of which can act directly or indirectly as electron donors to $BChl_2^+$. In *Rps. viridis* the electron transfer rates between the hemes and the $BChl_2$ are rapid, occurring into the sub-microsecond range [2].

In vivo, the re-reduction of $BChl_2^+$ by the cytochrome *c* in the periplasmic side of the membrane is followed by electron transfer from Q_A^- to the secondary quinone, Q_B, which in turn reduces the quinone pool at a point near the cytoplasmic side of the membrane. The vectorial location of the reducing and oxidizing parts of the electron transfer chain results in the generation of a transmembrane potential, ultimately coupled to solute transport and ATP synthesis [3].

A variety of techniques have been applied to study the electrogenic nature of the electron transfer reactions involved in the photosynthetic charge separation pro-

Abbreviations: LB, Langmuir-Blodgett; RC, reaction center; RC-cyt *c*, reaction center cytochrome *c* complex; LDAO, lauryldimethylamine *N*-oxide; β-OG, octyl-β-glucopyranoside; DPPC, L-α-dipalmitoylphosphatidylcholine; PL, phospholipid; Mops, 3-[*N*-morpholino]-propanesulfonic acid; Mes, 2-[*N*-morpholino]ethane sulfonic acid; DAD, 2,3,5,6-tetramethyl-*p*-phenylenediamine; TMPD, *N,N,N',N'*-tetramethyl-*p*-phenylenediamine; PES, *N*-ethylphenazonium ethosulfate; PMS, *N*-methylphenazonium methosulfate; DNAse, deoxyribonuclease; *o*-phen, 1-10-phenanthroline; DO, duroquinone; CAPS, (3-[cyclohexylamino]-1-propanesulfonic acid); Ches, (2-[*N*-cyclohexamino]ethanesulfonic acid).

Correspondence: G. Alegria, B501 Richards Building, Department of Biophysics and Biochemistry, University of Pennsylvania, Philadelphia, PA 19104, U.S.A.

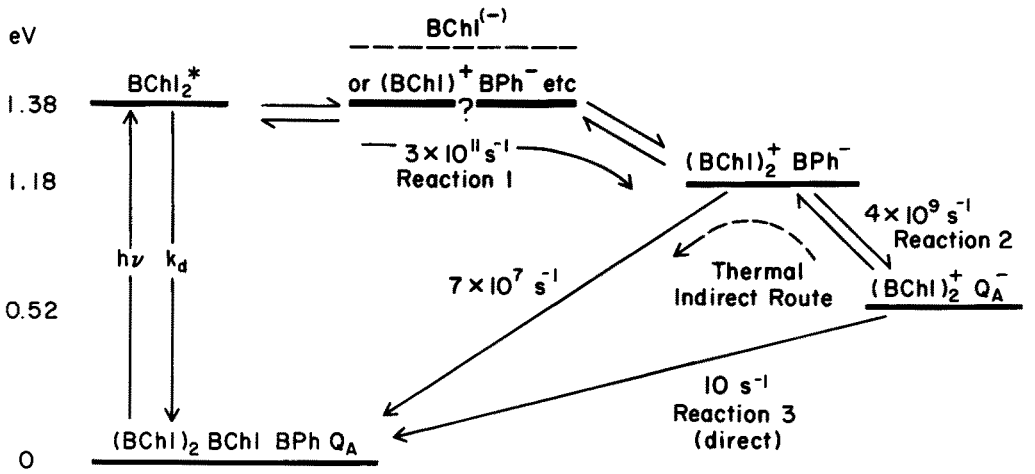

Fig. 1. Electron transfer pathways and energy levels in the isolated RC of *Rb. sphaeroides*. For simplicity the reactions involving Q_B as well as pathways yielding $BChl_2$ triplet states are omitted. The possible involvement of the monomeric BChl as an intermediate in the electron transfer from $BChl_2^*$ to BPh is illustrated. Reactions competing with the formation of the charge separated state $BChl_2^+ Q_A^-$ include: (a) decay of the excited state $BChl_2^*$ by fluorescence and non-radiatively (k_d) and (b) by direct charge recombination from $BChl_2^+ BPh^-$. Depending on the free energy gap between BPh and Q_A, the charge recombination process from $BChl_2^+ Q_A^-$ can occur via a direct process and by a thermally activated intermediate involving BPh.

cess with the intention of understanding the basis of the highly efficient energy transducing process (for a review see Ref. 4). We have considered that a very promising approach to the study of membrane redox proteins and the electron transfer processes they promote could be through construction and analysis of Langmuir-Blodgett (LB) monolayer films of the isolated RC proteins and of native photosynthetic membranes deposited on planar supports. However, it was clear from preliminary work [5,6] that optimization of the LB film technique as well as the development of analytical methods for a detailed characterization of the films were required before confidence could be placed on its general applicability. In this paper we describe fully the analytical methodologies involved and demonstrate that with the Langmuir-Blodgett technique it is possible to produce highly stable films in which the chromophores and redox cofactors of the photosynthetic process essentially retain their in vivo properties.

II. Materials and Methods

1. Chemicals

The following compounds, Mops, Mes, Tris-HCl, $CdCl_2$, $MgCl_2$, NaCl, $FeCl_2$, EDTA, sodium ascorbate, DPPC, arachidic acid, *o*-phen and DNAase were purchased from Sigma (St. Louis, MO). DEAE-cellulose was from Whatman (U.K.). LDAO and β-OG were from Calbiochem (La Jolla, CA). Compounds used as redox mediators were: DAD, TMPD, PMS, PES, pyocyanine, duroquinone, phenazine and ferrous-EDTA (1 : 2 molar ratios of $FeCl_2$: EDTA in water). The redox potentials were raised and lowered by small additions of well-buffered solutions of potassium ferricyanide and sodium dithionite respectively. The source of the redox mediators was Aldrich (Milwaukee, WI); other chemicals were commercial products of the highest purity available. The water used in the LB film work was deionized and doubly-distilled house water.

2. Biological materials

(a) Chromatophore membranes

Rps. viridis. Cells of *Rps. viridis* were grown in a modified Hutner medium [7] with malate as a carbon source and supplemented with *p*-aminobenzoic acid, thiamine HCl, nicotinic acid, 0.1% yeast extract and 0.01% casein. Approx. 50 g of wet cells were washed in 1 mM $MgCl_2$, 100 mM KCl, 20 mM Mops at pH 7.0. After DNAase treatment, the cells were broken by passage once through an Aminco French press cell disruptor (1200 psi) followed by sonication (3 × 15 s at maximum power) with a Branson Cell Disruptor-185. Cell debris was separated by centrifugation at 20000 × *g* for 10 min and the chromatophores were sedimented at 100000 × *g* for 60 min. The pellet was washed twice in 1 mM $MgCl_2$, 100 mM KCl, 1 mM Mes (pH 6.5). The optical absorbance of the final suspensions, measured at 1010 nm, was adjusted to about 60 for use in the preparation of LB films and 40 when used for the isolation of reaction centers. Chromatophore membrane LB films of improved quality were obtained using purified membrane suspensions. The purification procedure, essentially that reported by Jacob et al. [8], was as follows: the chromatophore suspension (A_{1015} 60) was overlaid onto a discontinuous sucrose gradient (0.5, 1.0, 1.5 and 2 M sucrose steps) in a 10 mM Tris-HCl buffer

at pH 8.0. After centrifugation at 140000 × *g* for 4 h using a Beckman SW-28 rotor, the enriched fraction was collected at the interface of the 1.0 and 1.5 M steps, sedimented by a 1 h spin at 100000 × *g* and resuspended in a 10 mM Tris-HCl (pH 8.0) buffer at final A_{1015} 50–60. Purified chromatophores were stored at 5 °C and used within 10 days after preparation.

Rb. sphaeroides. Chromatophores of the carotenoidless mutant *Rb. sphaeroides* R-26 were prepared essentially as described in Ref. 9. Suspensions of chromatophores in 10 mM Tris, 100 mM NaCl, 1 mM EDTA (pH 8.0) buffer were adjusted to an A_{850} of 50 for RC isolation.

(b) Isolation of reaction centers

Rb. sphaeroides. Reaction centers of *Rb. sphaeroides* R-26 were prepared from chromatophores as described previously [10]. The reaction centers were suspended in 0.1% LDAO, 10 mM Tris-HCl (pH 8.0) at concentrations of 30–50 μM. The purity of the preparations was determined by the 280 nm/800 nm absorbance ratio; this was typically 1.3. The activity of the preparations in solution was always higher than 90% (see the later section on spectroscopy for details). For the LB film work the LDAO was exchanged for β-OG or lipids (see section on detergent exchange, below).

Rps. viridis. Isolation and purification of *Rps. viridis* RC-cyt *c* complex from chromatophores was done essentially following a procedure developed by Pucheu et al. [11] as modified by Prince et al. [12]. The RC-cyt *c* complexes were suspended in 0.1% LDAO, 10 mM Tris-HCl (pH 8.0) at concentrations of 20–40 μM. The purity of the preparations was determined by the absorbance ratio at 280 nm/830 nm; this was 2.2–2.3. The activity, as determined by the cytochrome *c* photooxidation assay, was higher than 90% (see spectroscopy section for details). As with the *Rb. sphaeroides* RCs, LDAO was exchanged for β-OG or lipid prior to the formation of the LB films as described below.

(c) Detergent exchange

Films of *Rps. viridis* RC-cyt *c* complex were prepared from the protein solubilized in β-OG or reconstituted in lipid dispersions. In the case of *Rb. sphaeroides* RC dispersions in β-OG, although stable in solution, resulted in films with partially denatured protein; hence, for *Rb. sphaeroides* only RC reconstituted in lipid dispersions were used. However, both preparations involved exchange of LDAO for β-OG. This procedure was as follows: LDAO-solubilized reaction centers were loaded on a DEAE column and washed with approx. 1 liter of a detergent free buffer and then a buffer containing 30 mM β-OG, 10 mM Tris-HCl (pH 8.0). The RCs were eluted from the column with a 30 mM β-OG, 200 mM NaCl, 10 mM Tris-HCl (pH 8.0) buffer. This step resulted in an approx. 10% loss in yield but the activity of the preparations remained the same. Quantitative determinations of the efficiency of LDAO removal were not made, although the presence of small amounts of free LDAO were easily detected in the LB film balance; indeed this was used as a convenient criterion for optimization of the detergent exchange process (see below).

Freezing and thawing of RCs in β-OG resulted in unstable and eventually denatured films, even for the *Rps. viridis* RC-cyt *c* complex and hence β-OG dispersions were stored at 5 °C. It was common to use the preparations within 10 days of isolation.

(d) Reaction centers in phospholipids

Reaction center-phospholipid dispersions (hereafter referred to as PL : RC dispersions) of both bacterial species were prepared replacing the β-OG by phospholipids. The procedure was essentially as reported previously [1]: DPPC was added to the β-OG solubilized RCs in a DPPC : RC ratio of 80–200 : 1 (*Rps. viridis*) and 150–400 : 1 (*Rb. sphaeroides*), the lipid-protein mixture was dialyzed overnight against a 10 mM Tris-HCl buffer at pH 8.0 at 5 °C to remove the β-OG. The efficiency of the removal was not quantitated. The PL : RC dispersions were kept at 5 °C and were used within 1 week after preparation.

3. Langmuir-Blodgett films

A Langmuir-Blodgett film balance (Lauda Type 1974; Sybron/Brinkmann, Westbury, NY) was used to make the films following the general procedure described elsewhere [13,14]. However, substantial modifications have been made that have resulted in an improvement of the film quality. These are described below.

(a) Subphase conditions

For preparation of films of isolated RCs in detergent or lipid the film balance trough contained an aqueous solution of 2 mM $CdCl_2$, 2 mM ascorbate, 10 mM Tris-HCl at pH 8.0, whereas for films of chromatophore membranes the subphase contained 2 mM $CdCl_2$, 2 mM ascorbate, 2 mM Mes at pH 6.5. All films were made under an argon atmosphere; the subphase temperature was adjusted to 10 °C (±2). The presence of ascorbate in the subphase to provide reducing conditions prevented a 10% to 20% loss of photo-activity in the RCs on the deposited LB films.

(b) Spreading conditions

Both RCs and chromatophores were spread at the gas/water interface using the 'glass-rod' method [15]. This involved placing a 0.6 mm diameter glass rod at a small angle (< 300) relative to the trough plane positioned so that it just touched the water surface. 2 μl aliquot amounts of material were spread at the interface

via the rod, waiting approx. 10 s between additions; during this procedure the trough surface area was held constant.

The behavior of both types of preparation (RCs and chromatophores) at the interface was monitored by measuring (i) the final surface pressure promptly after spreading was completed, and (ii) the ensuing rate of change of the surface pressure measured on a minutes time-scale. These two assays provided a good prognosis of the quality of the deposited films to be produced later. For instance, films at the interface exhibiting final pressures above 5 mN/m correlated with films showing poor orientation. Another negative sign was an increase of interface pressure of more than 2 mN/m occurring over a period of 1 min after addition; such change indicated loss of activity due to protein denaturation (see Spectroscopy section, below, for details).

For the preparation of films of isolated RCs both in lipid and β-OG, best results were obtained with (i) initial spreading densities of 10^{10} RCs per cm^2, (ii) preparations that generated less than 5 mN/m surface pressures at this initial density and (iii) subsequent pressure increase rates of less than (0.2 mN/m)/s. As mentioned before, LB films of *Rb. sphaeroides* RCs in β-OG resulted in variable degrees of protein denaturation and hence for this species best results were obtained with PL : RC dispersions. In contrast *Rps. viridis* RC-cyt *c* complexes in β-OG and in lipids resulted in comparable LB film quality.

In the case of chromatophores, optimal deposited film quality was obtained by spreading 30–40 μl of chromatophore suspension (*A* of 60 at 1010 nm) to an initial area of 500 cm^2. Under these conditions the final surface pressure remained below 1 mN/m and increased at a rate of less than 0.2 mN/ms. Preparations which did not satisfy these criteria were discarded.

(c) Compression rates and film stability

After the spreading procedure was completed and found to conform to the above quality requirements, the films at the interface were compressed at a speed of 6 cm/min and the increase in surface pressure monitored as the film approached the closed-packed state. When the pressure reached a value of 25 mN/m the compression was stopped and the film stability checked by measuring the change of area as a function of time while maintaining a constant pressure of 25 mN/m. Films of both isolated RCs and chromatophores showing variations in area of less than 1.4% change of the initial area per hour under these conditions were considered suitable for deposition onto a solid support. Area *increases* exceeding this value produced deposited films with partially denatured protein.

Unstable films exhibiting fast area *decreases* (e.g., 10%/h) at 25 mN/m constant pressure were commonly obtained with LDAO-solubilized RCs. In these cases the shape of the pressure versus area curve during the compression procedure (compression isotherm) is almost identical to that of a film made with protein-free solution of 0.1% LDAO. We associate the low stability of these preparations with the formation of LDAO-RC micelles that sink into the subphase. When deposited onto solid supports, these films exhibited good activity but had little or no orientation. However, this problem was not observed with RC preparations in which the LDAO was exchanged for β-OG. It is worth mentioning that if the exchange of LDAO for β-OG in the RC suspension was insufficient, the LDAO could be readily detected in the pressure/area curve. As a general rule decreasing areas at constant pressure of more then 1.4%/h were taken as a prognosis for poorly oriented films when subsequently deposited on solid support. These preparations were discarded.

(d) Substrate preparation and film deposition

Glass and quartz slides (Spectra-Cell, Oreland, PA) were washed with a phosphate-free detergent, thoroughly rinsed with distilled water, soaked in chromic acid for 1 h and thoroughly rinsed again in distilled water. The cleaned slides were used immediately. In preparation for the deposition of a film, the slide was mounted on a home-made dipper with its plane at 90° to the gas/water interface. The slide was inserted at a relatively fast speed (10 mm/s) into the water phase and through the interfacial film made as described above and maintained at a pressure of 25 mN/m. This speed of entry through the film into the water phase caused no detectable depositions of either RCs or chromatophores as indicated by the absence of a change in the film area. The submerged slide was then withdrawn at 0.15 mm/s while keeping the surface pressure constant. The amount of material removed from the gas/water interface was measured from the decrease in the surface area. The ratio of coated area on the slide and the decrease in the film area in the trough provided the deposition ratio; this was typically 0.96. Multilayers of both RCs and chromatophores could be built up by repeating the process with no appreciable change in deposition ratio provided the down stroke entry into the subphase was done at approx. 10 mm/s; any peeling off of previous depositions that did occur was detectable as an increase in the film area (at constant pressure) as the slide passed through the interface. Typically one trough loading (approx. 500 cm^2) was used to make up to 7 depositions.

Irregularities introduced in the build-up of multilayers on the substrate were checked by measuring the increments in absorbance (see Materials and Methods section (4a) and Results) and loss of orientation per deposition (see section (2a) of Results and accompanying paper [51]). These assays showed that up to 35 monolayers could be built up with little change in the

quality of deposition and orientation as compared to that displayed by a single monolayer.

(e) Arachidate film coatings

The chromatophore films prepared as described above were routinely coated further with arachidate monolayers. Arachidate films were spread using the same subphase as that used with chromatophores except that no ascorbate was added and the temperature was 20 °C. Arachidate monolayers were formed by adding 30 μl of a 10 mM arachidate solution in hexane at 500 cm^2 trough area. After 10 min to allow evaporation of the solvent, the film was compressed to 30 mN/m for deposition. Three to five arachidate monolayers were deposited on top of the chromatophore films. This procedure effectively prevented loss of the deposited chromatophore films from being washed off when submerged in buffer. For instance, without the protective coating a monolayer of chromatophores bathed in water moderately stirred as required for redox equilibration would wash off on a 1–2 h time-scale. This washing off problem appeared confined to LB films of native membranes; thus for isolated RC films the arachidate coatings were not applied.

4. Redox potentiometry

Redox titrations of the redox centers in the isolated RC and in the chromatophore deposited films were performed anaerobically in the redox cuvette illustrated in Fig. 2. The redox mediators and procedures were essentially as previously described [16]. The redox potential was measured with a micro-combination platinum-calomel electrode (Microelectrodes, Londonderry, NH). In all of the redox titrations the solutions contained 20–30 μM concentrations of mediators. The time allowed for redox equilibration was routinely 10 min. All the titrations reported were performed with at least three different films performed in both reductive and oxidative directions. For all the redox cofactors

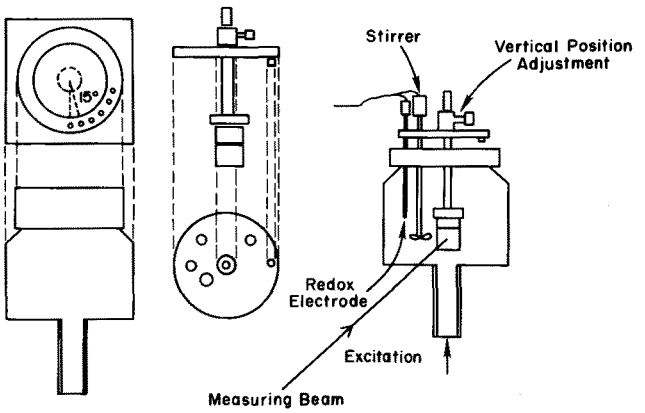

Fig. 2. Apparatus for redox potentiometry and spectrophotometry of LB films.

titrated, the maximal standard deviations in midpoint potentials from three independent determinations were less than 20 mV. For simplicity, uncertainties will be omitted.

In the case of arachidate coated films we observed that the hydrophobic character of a freshly coated sample was altered at the end of the redox titration when a small fraction of the total surface appeared wet. This indicated that either partial or total peeling off of the fatty acid coating had occurred in those places leaving the chromatophore film exposed. We think that good redox mediation in arachidate coated samples is achieved through the formation of small holes in the fatty acid multilayer. However, the partial loss of the protecitve layer had no consequences on the orientation of the chromatophores membranes on the slide.

5. Spectroscopy

(a) Absorption spectra

Absorption spectra of the deposited films on quartz or glass slides were recorded using a computer controlled, chopped dual wavelength spectrophotometer (Biomedical Instrument Group, University of Pennsylvania) equipped with a scanning device and a photodiode detector operating over the range 400–1200 nm. Digitized spectra were stored and manipulated for baseline corrections using a program designed by Mr. Stephen Leo of the Biomedical Instrumentation Group at the University of Pennsylvania.

The experimental arrangement for taking spectra of the LB films at defined redox potentials is shown in Fig. 2. The sample was mounted vertically in the slide holder and the angular position of the slide relative to the measuring beam adjusted by inserting the pin in one of the holes placed at 150 intervals in the cuvette top. The 90° position of the slide was calibrated by placing a mirror in the sample holder and rotating it about the vertical axis until the beam exactly overlapped with its image. Oxygen was removed from the bathing solution by pushing the gas inlet into the liquid and bubbling with argon for at least 2 h. During the redox titration the gas pipe was kept above the bathing solution level with the flow adjusted to maintain the interior slightly above atmospheric pressure. The redox electrode and stirrer entered the solution from the top as shown in Fig. 2. Redox mediators were then added via a syringe through a septum and the potential was adjusted to the required value.

Since redox dyes undergo considerable redox dependent spectral changes, at each redox potential a reference spectrum was taken by placing the sample holder in its lowest position so that the spectrophotometer beam passed through the upper, uncoated part of the slide; in this way a spectrum of the glass substrate and bathing solution containing colored redox mediators

was obtained. The film spectrum was then taken at the same potential by raising the sample holder to the highest position where the beam passed through the lower coated part of the slide. This procedure was facilitated by a sliding mechanism in the sample holder which allowed adjustment of the vertical position of the sample without changing the angle between the plane of the slide and the measuring beam. Furthermore, since the same piece of glass substrate was used throughout the measurement of experimental and reference spectra, artifacts introduced by variations in the optical properties of different pieces of substrate were eliminated. At each potential, subtraction of the two spectra revealed the changes occurring in the deposited film. The area of the measuring beam was approx. 0.5 cm^2. Unless otherwise specified, all absorption spectra were taken with the slide plane at 30° to the measuring beam corresponding to an angle of incidence of 60°, measured relative to the normal of the slide.

All spectra were taken with the LB films immersed in a redox buffer containing 60% glycerol chosen to match the index of refraction of the substrate and the bath. This minimized scattering and reflectance effects that appear as typical dispersive distortions in the baseline when the spectra are measured with the slide immersed in water.

The orientation of the reaction center and chromatophore membrane LB films was determined using linearly polarized absorption spectroscopy. Polarized absorption spectra were measured using the same geometry as explained above. A Nicole prism (Oriel, Stratford, CT) placed in the beam path before the sample was the source of polarized light. The direction of polarization was changed by rotation of the polarizer without disturbing the position of the slide. A more detailed experimental and theoretical analysis of the LB film orientational properties is presented in the accompanying paper [51].

(b) Kinetic measurements

Light-induced absorbance transients were measured in an unchopped dual wavelength spectrophotometer (Biomedical Instrument Group, University of Pennsylvania) used in the single beam configuration. For measurements in the visible, the actinic light was a xenon flash lamp (10 μs full width at half maximum) filtered with an infrared transmitting Kodak 88A wratten filter; the light intensity in this arrangement was sufficient to activate approx. 95% of the reaction centers. For measurements of absorption transients in the near IR the actinic light was filtered with a blue glass filter (Kodak 38) with low red and IR transmittance. The photomultiplayer tube (S1 type) was protected with interference filters (Oriel) with maximum transmittances at 860 nm and 960 nm. In this configuration the light intensity was 60% saturating. The deposited films were photoactivated using a light pipe placed at the bottom of the cuvette as shown in Fig. 2. For this purpose the slide was mounted so that the plane made either a 30°, 45° or a 60° angle to the excitation pulse and a 60°, 45° or 30° angle to the measuring beam, respectively. Checks for contributions to the transients from stray light due to reflections of the excitation beam in the slide were made routinely by flashing blank slides. Absorbance transients were stored and averaged using a Computerscope (RC-Electronics, Santa Barbara, CA). Determination of rate constants and ampitudes were done using the ASYSTANT + software package (ASYST Software Technologies, Rochester, NY). For this purpose the kinetic transients were averaged between 20 and 30 times. The uncertainty limits are standard deviations over at least four different samples.

(c) Functional assays

(i) Activity of the isolated RCs. The activity of the *Rb. sphaeroides* preparations in solution and in the LB films was determined by the ratios of the absorbance at 800 nm (RC concentration) and the light-induced absorption changes associated with the formation of $BChl_2^+$ at 860 nm (extinction coefficients of 288 $mM^{-1}\,cm^{-1}$ and 128 $mM^{-1}\,cm^{-1}$, respectively [17]). For the *Rps. viridis* RC-cyt *c* complexes in solution and in LB films, the activity was determined by the ratios of absorbance at 830 nm (RC concentration; 300 $mM^{-1}\,cm^{-1}$ [18]) and the light-induced absorbance decrease measured at 558 nm for the cytochrome *c* oxidation (20 $mM^{-1}\,cm^{-1}$ [18]). For these assays the preparations were poised at a redox potential of 200 mV to make certain that the cytochrome *c* is reduced prior to excitation. Kinetics of charge recombination from the states $BChl_2^+Q_A^-$ and $BChl_2^+Q_B^-$ in isolated RC-cyt *c* complex LB films were measured at 450 nm, a wavelength containing contributions from both $BChl_2^+$, Q_A^- and Q_B^- [19]. The same reactions in chromatophore LB films were monitored at near-infrared absorption band of $BChl_2^+$ at 960 nm (123 $mM^{-1}\,cm^{-1}$ [18]). For both species the percentage of Q_B activity was determined from the ratio of the fast and slow components in the charge recombination measurements.

(ii) Redox analysis of $BChl_2$. $BChl_2$ was measured in the isolated RCs by monitoring the absorption at 860 nm for *Rb. sphaeroides* and at 960 nm for *Rps. viridis*.

(iii) Redox analysis of the primary quinone Q_A. The redox state of the primary quinone in *Rb. sphaeroides* RCs was monitored indirectly by measuring the light-induced decrease in absorption at 860 nm that accompanies stable formation of $BChl_2^+Q_A^-$. Since under the conditions of our measurements the extent of stable (milliseconds) $BChl_2$ photo-oxidation is limited only by the concentration of RCs containing oxidized quinone Q_A, the amplitude of flash generated $BChl_2^+$ can be used to determine the redox state of Q_A. For the *Rps.*

viridis RC-cyt *c* complex a similar indirect assay was used with the exception that the amplitude of photo-oxidized cytochrome *c* was measured to indicate the state of Q_A reduction as a function of redox potential. Thus, if Q_A is in an oxidized state and at least one cytochrome *c* is reduced prior to excitation, a flash generates maximum yield of the state (cyt *c*)$^+$BChl$_2$Q$_A^-$, which is stable for several seconds. If, on the other hand, Q_A is in the reduced state before excitation, the flash activated precursor BChl$_2^+$BPh$^-$ recombines in nanoseconds, faster than electron donation from the cytochrome *c* can form significant levels of the state (cyt *c*)$^+$BChl$_2$ BPh$^-$, and no cytochrome *c* photo-oxidation will be observed. Since the amplitude of the photo-oxidized cytochrome *c* is only limited by the concentration of RC with Q_A in the oxidized state, the extent of cytochrome *c* photooxidation can be used to determine the redox state of Q_A.

(iv) Redox analysis of the cytochromes. The four cytochrome *c* hemes in the *Rps. viridis* RC-cyt *c* complex were analyzed using the absorbance of the α-bands characteristic of the reduced form of each individual heme in the 550–570 nm region referred to a reference wavelength at 540 nm. Further details of the spectral resolution of each heme will be described in the Results and Discussion sections.

III. Results

1. LB films at the air/water interface; compression isotherms

The behavior of β-OG : RC, DPPC : RC dispersions and chromatophore membranes at the air/water interface is illustrated in Fig. 3. The isotherm for the pure lipid (A) shows the typical features of good LB film forming molecules; this includes the near-zero initial surface pressures indicative of a gas phase, and sharp pressure increments during compression interpreted as gas-liquid-solid-like phase transition [20]. The break at approx. 12 mN/m has been identified as a solid/liquid phase transition. These features are also apparent in the isotherms for the 400 : 1 DPPC : RC dispersion (B), indicating that at this protein content the phase behavior of the lipid is essentially retained. This interpretation is supported by the temperature dependence of the isotherms of the PL : RC dispersions which in the range $10\,°C < T < 25\,°C$ exhibit phase transition properties similar to those of the pure lipid (data to be presented elsewhere). Except for the position of the break in the slope, the shape of the isotherms for both pure lipid and PL : RC dispersions remained essentially unchanged for compression speeds ranging from 0.1 to 10 cm/min. In Fig. 2B the reproducibility of the isotherms for one preparation is illustrated by the continuous and dashed lines; we find that the major source of variability arises from a lack of control over the efficiency of the spreading process. In (C), isotherms of PC : RC dispersions of *Rps. viridis* RC-cyt *c* complex exhibit sharper slopes than β-OG : RC dispersions. This appears to correlate with slightly improved oriented films using PC : RC dispersions. Isotherms of *Rps. viridis* chromatophore membranes (D) show similar characteristics to those of 400 : 1 PC : RC dispersions; however, due to the heterogeneity in the lipid and protein composition, the fluid-solid phase transition has disappeared. Chromatophore membranes of *Rb. sphaeroides* exhibit similar behavior.

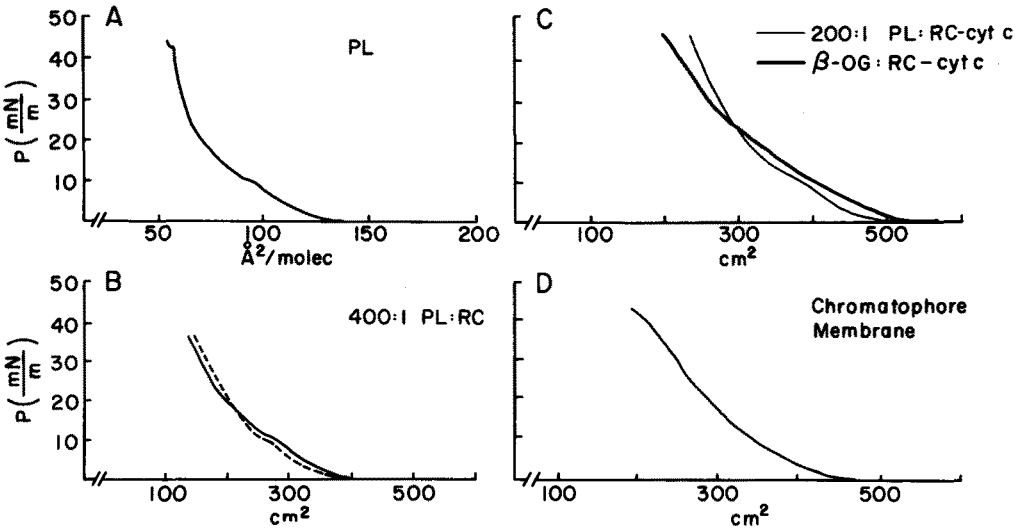

Fig. 3. Compression isotherms of the preparations used for LB film depositions. (A) Pure phospholipids, addition of $3.15 \cdot 10^{16}$ molecules of DPPC dissolved in chloroform at an initial area of 500 cm^2. (B) 400 : 1 PL : RC dispersion of *Rb. sphaeroides*: both curves correspond to additions of $1.84 \cdot 10^{14}$RC molecules and $7.35 \cdot 10^{16}$ PC molecules at 500 cm^2 initial area. (C) (———) 200 : 1 PL : RC-cyt *c* complex from *Rps. viridis*: addition of $1.5 \cdot 10^{14}$ RC-cyt *c* complex molecules and $3 \cdot 10^{16}$ PC molecules at same initial area as in (B), (_____) β-OG : RC-cyt *c* complex from *Rps. viridis*: addition of $5 \cdot 10^{14}$ RC-cyt *c* complex molecules at same initial area as before. (D) *Rps. viridis* chromatophore membranes: addition of 40 μl of chromatophores (*A* of 60 at 1015 nm) at same initial area as before. Subphase temperature 10 °C (±2).

We also examined the compressibility and stability properties of films of detergent-protein dispersions using different detergents (data not shown). It was observed that the quality of the deposited RC films improved with increasing detergent critical micelle concentration (CMC). Marked improvements were encountered in the film compressibilities and stabilities at the interface, and in the spectral quality and orientation of the deposited films using the series of detergents Triton X-100 (CMC 0.24 mM), LDAO (2.2 mM), sodium cholate (13 mM) and β-OG (25 mM).

2. Characterization of the isolated RC films

(a) Spectral quality and photo-activity of the LB films

Fig. 4 shows absorption spectra of multilayer films of *Rps. viridis* in β-OG (A) and of *Rb. sphaeroides* in lipids (B) deposited at a surface pressure of 25 mN/m. In both cases spectra of the same preparations in solution are shown for comparison. To aid the comparison the spectra were normalized at the maximum in the near-infrared absorption band of $BChl_2$ (960 nm for *Rps. viridis* and 860 nm for *Rb. sphaeroides*). From the figure it is clear that for both species the RC protein as a deposited film retains a close similarity to the native spectra. However, minor but clearly identifiable differences are apparent: in both cases there are blue shifts of the bands associated with $BChl_2$ as well as decreases in the absorption maxima of the monomeric bacteriochlorophyll BChl (at 830 nm in *Rps. viridis* and 800 nm in *Rb. sphaeroides*). The small differences in peak amplitudes between the two spectra can be ascribed to preferential absorption in the LB films arising from the partial polarization of the measuring beam and the orientation of the RC protein. Fig. 5 shows typical polarized absorption spectra of a multilayer of a 400 : 1 DPPC : RC dispersion from *Rb. sphaeroides*. It is clear that the absorbance in the bands associated with the chromophores in the RC protein strongly depends on the direction of polarization. A quantitative analysis of the spectra of LB films of both bacterial species indicates that the symmetry axis of the RC protein is preferentially oriented perpendicular to the plane of the slide (see accompanying paper [51]).

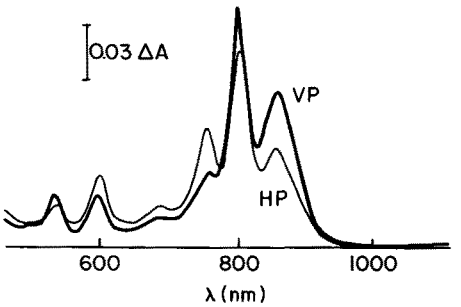

Fig. 5. Polarized absorption spectra of a 15-layer LB film of a 400 : 1 DPPC : RC dispersion from *Rb. sphaeroides*. Vertical polarization (_____), horizontal polarization (———). The slide was immersed in a 60% glycerol, 10 mM Tris (pH 8.0) buffer with 2 mM ascorbate. Same geometry as in Fig. 4.

Calculations of the protein density in the LB films from the absorbance at 800 nm (assuming ε remains at 288 $mM^{-1}\,cm^{-1}$) and at 830 nm (ε 300 $mM^{-1}\,cm^{-1}$) for the *Rb. sphaeroides* and *Rps. viridis* RCs respectively yielded roughly similar values; for DPPC : RC ratios of 400 : 1 and 200 : 1 typical densities were $0.8 \cdot 10^{12}$ and $2 \cdot 10^{12}$ RC/cm^2 per monolayer, respectively. These values are in agreement with those reported for *Rb. sphaeroides* RCs reconstituted into phospholipid monolayers preformed at the air/water interface with PL : RC ratios of 100 : 1 [21,22]. Maximal uncertainties in these values were of 25–30%, due mostly to lack of control in the spreading efficiency. Higher protein densities could be achieved by depositing the films at higher surface pressures (above 30 mN/m); however, spectroscopic analysis revealed loss of orientation (data not shown). Optimal protein densities and orientations were obtained in the range from 25 to 30 mN/m. DPPC : RC ratios in the deposited films were not de-

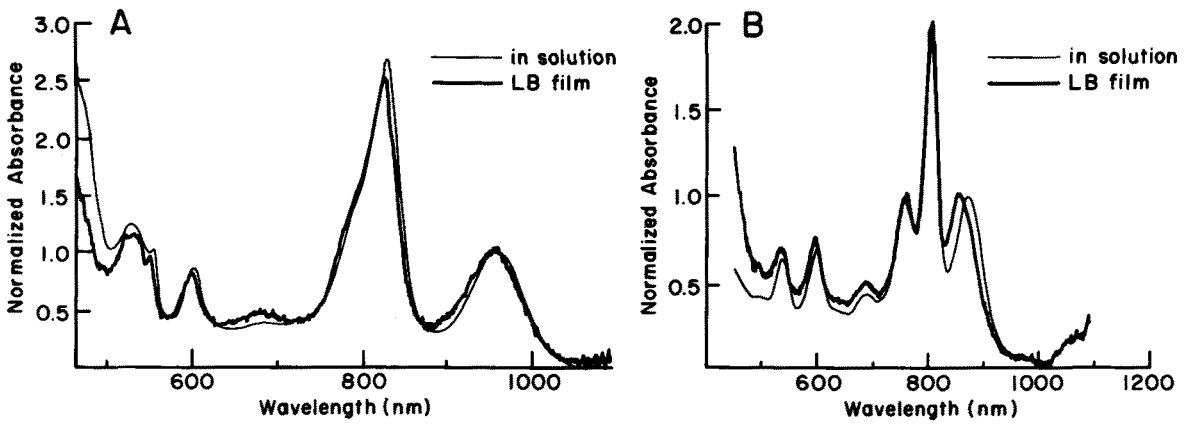

Fig. 4. (A) Absorption spectra of a β : OG dispersion of *Rps. viridis* RC-cyt *c* complex in solution (———) and in a 14-layer LB film (_____). The spectra were normalized at 960 nm. (B) Absorption spectra of a PL : RC dispersion of *Rb. sphaeroides* in solution (———) and in a 14 layer film (_____). The spectra were normalized at 860 nm. In both A and B the LB film spectra were obtained with the slide plane at 30° to the measuring beam in a 60% glycerol (pH 8.0) redox bath contained 20 μM DAD and the potential adjusted to 200 mV with sodium dithionite.

termined; however, it was observed that above 100:1, the concentration of RCs on the slide decreased approximately proportionally with the increase of DPPC:RC ratio, indicating that the molar ratio of the dispersions in solution was preserved at the interface.

The activity of the RC protein in the LB films from both *Rb. sphaeroides* and *Rps. viridis*, assayed as described in Section 5c of Materials and Methods, indicates that an apparent loss of about 20–30% is incurred relative to its value in solution. Since the activity assay for *Rps. viridis* measures photo-oxidizable cytochrome *c*, we have considered whether the lower activity may have arisen from a dissociated or dysfunctional cytochrome *c* subunit in the LB film. However, we find no detectable amount of the oxidized $BChl_2$ that should be stably formed after the flash if this was the case. Thus severe disruption of the cytochrome *c* subunit can be ruled out as the cause for activity loss. The possible sources of this apparent loss of activity are discussed later.

The spectral quality, orientation and activity of fresh LB films as described above are retained for months after preparation when stored in the dark at 5°C.

(b) Kinetics of electron transfer involving Q_A and Q_B

The kinetics of charge recombination from the charge separated state $BChl_2^+Q_A^-$ or $BChl_2^+Q_B^-$ were measured in multilayer LB films of both bacterial species. In the case of *Rps. viridis* it was necessary to oxidize the four cytochrome *c* hemes before excitation, otherwise a ferrocytochrome *c* would reduce $BChl_2^+$ before either Q_A^- or Q_B^-. Use of ferricyanide to oxidize the hemes was avoided because it is known to interact with the light-induced Q_A^- leading to a near irreversible photo-oxidation of $BChl_2$ [23]. Instead, the cytochromes were oxidized by exposing the deposited film to atmospheric oxygen for about 10 min. An absorption spectrum of the film proved that this was an effective procedure to oxidize the cytochrome *c* complement without oxidizing $BChl_2$.

Fig. 6 shows the flash activated kinetics of the absorption change at 450 nm in a multilayer LB film of *Rps. viridis* with no reduced cytochromes before excitation. This transient was fitted with two exponentials: a fast phase with rate constant of 115 s^{-1} (60% of the total amplitude) and a slow phase with a rate constant of 4.5 s^{-1} (40% contribution). We observed preparation dependent variations in the rate of the fast component of ±20% and of ±10% in the slow phase; the reason for this difference is not clear. Both components have somewhat slower rates than those reported for the charge recombination from $BChl_2^+Q_A^-$ and $BChl_2^+Q_B^-$ in RC-cyt *c* complex in solution (346 s^{-1} and 6.3 s^{-1}, respectively [24]). The percentages of slow phase, which depend on Q_B occupancy as well as the free energy difference between Q_A and Q_B (see Discussion), were observed to

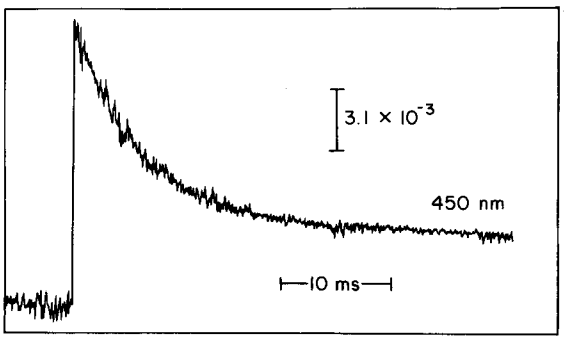

Fig. 6. Light-induced absorption changes at 450 nm on a 14-layer LB film prepared from a β:OG dispersion of *Rps. viridis* RC-cyt *c* complex. The cytochrome *c* hemes were oxidized by a 10 min exposure of the film to atmospheric oxygen. The slide was placed at 45° to both excitation and measuring beams in a 60% glycerol (pH 8.0) bath. No redox mediators were added. The transient kinetics were fitted with two exponentials with rates of 115 s^{-1} (60%) and 4.5 s^{-1} (40%).

be constant for films made from the same preparation but varied from 35% to 45% for different preparations.

Fig. 7 shows that the RC-cyt *c* complexes in the film retain Q_B function and hence are able to perform double turnovers when the cytochrome *c* complement contains two reduced hemes prior to excitation. In this experiment the sample was poised at a redox potential of 200 mV, where the two highest potential hemes are close to a 100% state of reduction prior to activation. It is clear that upon a second saturating flash the extent of additional cytochrome *c* photo-oxidation is 60% of that seen on the first flash. This result is consistent with the presence of active secondary quinone Q_B; however, the second flash oxidation appears to exceed the typical 35% to 45% occupancy of Q_B deduced from the kinetics of charge recombination. The difference arises from at least two contributions: (a) the measuring wavelength is at the absorption maximum of the heme oxidized on the second flash (see Fig. 14); (b) the partial polarization of

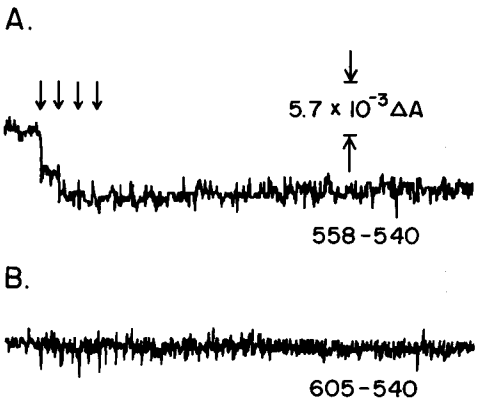

Fig. 7. (A) Light-induced cytochrome *c* oxidation of a multilayer LB film from a β:OG dispersion of *Rps. viridis* RC-cyt *c* complex poised at a redox potential of 200 mV. The redox bath contained 20 μM DAD. The arrows represent four successive flashes. (B) Photo-response of the film at 605 nm under the same conditions as in (A).

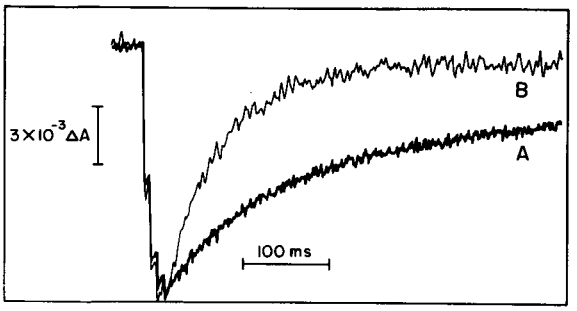

Fig. 8. (A) Light-induced absorption changes at 860 nm in a ten-layer LB film prepared from a 400:1 PL:RC dispersion of *Rb. sphaeroides* RCs. The slide plane made a 45° angle with the measuring and excitation beams. Excitation with blue light was approx. 60%. Redox bath conditions as in Fig. 5C. The kinetics were fitted with a two-exponential curve with rates 9.9 s^{-1} (30%) and 0.77 s^{-1} (70%). (B) Same as in (A) but in the presence of 3 mM *o*-phen. The data were fitted with a single exponential with rate constant of 10.6 s^{-1}.

the measuring beam and the different orientation of the two high-potential hemes result in different apparent extinction coefficients (see accompanying paper). Fig. 7B shows that no absorption changes associated with the photo-oxidation of $BChl_2$ were detectable in the time-scale of the measurement, which, as mentioned before, indicates that all functional RCs possess functional cytochromes. Use of the inhibitor *o*-phen to prevent the Q_A to Q_B electron transfer and thus confirm the presence of Q_B activity unfortunately was not an option because we found that it caused irreversible damage to the RC film. The reason for the damage to *Rps. viridis* by *o*-phen is not understood; however, this effect was not observed with *Rb. sphaeroides* LB films (see below).

Fig. 8 shows the light-induced absorption changes in a multilayer of a PC:RC 400:1 LB film of *Rb. sphaeroides* measured at 860 nm in the absence and presence of *o*-phen. In the absence of *o*-phen (trace A) the kinetics of charge recombination show a biphasic behavior with rate constants of 99 s^{-1} and 0.77 s^{-1} (±10%) with 30% and 70% contributions to the total amplitude respectively. These values are in good agreement with those reported for RCs in solution for the charge recombination processes from $BChl_2^+Q_A^-$ and $BChl_2^+Q_B^-$, respectively (rate constants of 7 s^{-1} and 0.7 s^{-1} [25]). The percentages of slow phase were preparation dependent and ranged from 60% to 70%. In the presence of approx. 3 mM *o*-phen (trace B), the kinetics exhibit a 95% fast phase with a rate constant of 10.65 s^{-1}. This demonstrates the functionality of the Q_A to Q_B electron transfer in the LB film and its sensitivity to *o*-phen.

(c) Equilibrium redox characterization of the chromophores in the RC deposited films

Redox characterization of $BChl_2$ and the primary quinone Q_A were performed in LB films of *Rb. sphaeroides* RCs prepared from PL:RC dispersions. Work with *Rps. viridis* was done on LB films of RC-cyt *c* complex made with three types of preparation: LDAO:RC-cyt *c*, β-OG:RC-cyt *c* and PC:RC-cyt *c* dispersions. The titrations of $BChl_2$, Q_A and the four cytochrome *c* hemes were done on LB films of β-OG:RC-cyt *c* complex. The hemes were also titrated in LB films prepared from RC-cyt *c* dispersions of LDAO and PL. Titrations of Q_A and $BChl_2$ in detergent dispersions in solution were done for *Rps. viridis*, since the midpoint potentials reported in the literature are limited to measurements in chromatophores.

(i) Midpoint potential of $BChl_2$. A redox titration of $BChl_2/BChl_2^+$ in the *Rps. viridis* RC-cyt *c* complex in solution and in a multilayer film is shown in Fig. 9A. The variable in the ordinate is the absorbance at 960 nm referred to its maximum fully reduced value at 200 mV. The titration data are fit to a single Nernst curve for a one-electron ($n = 1$) redox reaction with a midpoint potential, E_{m8} of 464 mV. Fits to the data in solution gave an identical midpoint.

Fig. 9B shows absorption spectra of the film at 200

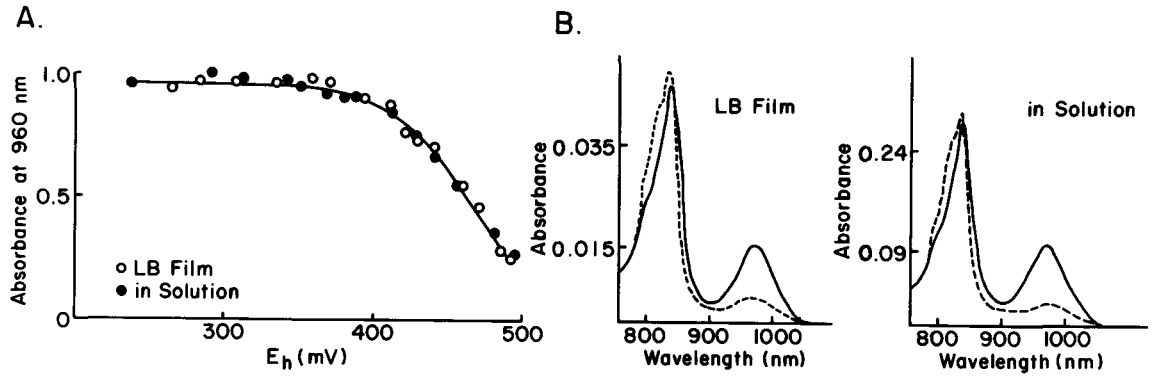

Fig. 9. (A) Redox titration of the bacteriochlorophyll dimer $BChl_2$ in a ten-layer LB film prepared from a β:OG dispersion of Rps. virdis RC-cyt *c* complex (○) and of the same preparation in solution (●). In both cases the medium was a 60% glycerol, 10 mM Tris-HCl (pH 8.0) buffer. The titrations were performed without redox mediators. For the LB film titration the slide was placed vertically at an angle of 45° to the measuring beam. The vertical axis shows the absorbance at 960 nm normalized at its maximum value at 200 mV. The continuous line is a fit with an $n = 1$ Nernst curve having a midpoint $E_{m8} = 464$ mV. (B) Absorption spectra of the samples used for the redox titration in the LB film and in solution. The spectra with continuous lines were obtained at 200 mV and those in dashed lines at 490 mV.

mV and 490 mV (dashed and continuous line, respectively on the left panel). The corresponding spectra in solution at the same redox potentials are shown in the right side panel. In addition to the bleaching of the 960 nm band, the well-known spectral changes in the 830 nm band associated with the formation of $BChl_2^+$ are apparent in both spectra [26].

Fig. 10A shows the corresponding titration of $BChl_2/BChl_2^+$ in a multilayer film of *Rb. sphaeroides*. In this case the ordinate is the absorbance at 860 nm relative to its maximum value at 200 mV. The fit to the data yielded an E_{m8} value of 414 mV. Fig. 10B shows absorption spectra of the LB film poised at redox potentials (E_h) of 188 mV and 441 mV. Again, the well characterized spectral changes associated with the formation of $BChl_2^+$ are apparent: bleaching of the 860 nm band and electrochromic shifts in the BPh band at 760 nm and the monomeric BChl at 800 nm [27].

(ii) Midpoint potential of the primary quinone, Q_A, and its pH dependence

Fig. 11A shows a typical redox titration of Q_A^-/Q_A in the *Rps. viridis* RC-cyt *c* complex in solution and in a multilayer film. The ordinate is the amplitude of the light-induced cytochrome *c* oxidation normalized to its maximum value at E_h 200 mV where Q_A is fully oxidized. The continuous and dashed lines are one-electron Nernst curve fits to the data: for the RC-cyt *c* complex in the deposited film the midpoint potential E_{m8} value is −165 mV and for the RC-cyt *c* complex in solution the E_{m8} value is −135 mV. The 30 mV shift that we obtain between the LB film and the RCs in solution was reproducible and is outside of the range of maximal experimental uncertainty (±20 mV). In Fig. 11B cytochrome *c* photo-oxidation at 551 nm at −20 mV for RCs in an LB film and in solution are presented; it is clear that in both cases the flash oxidized cytochrome exhibits a very similar slow time course of re-reduction indicating similar functional conditions in both systems.

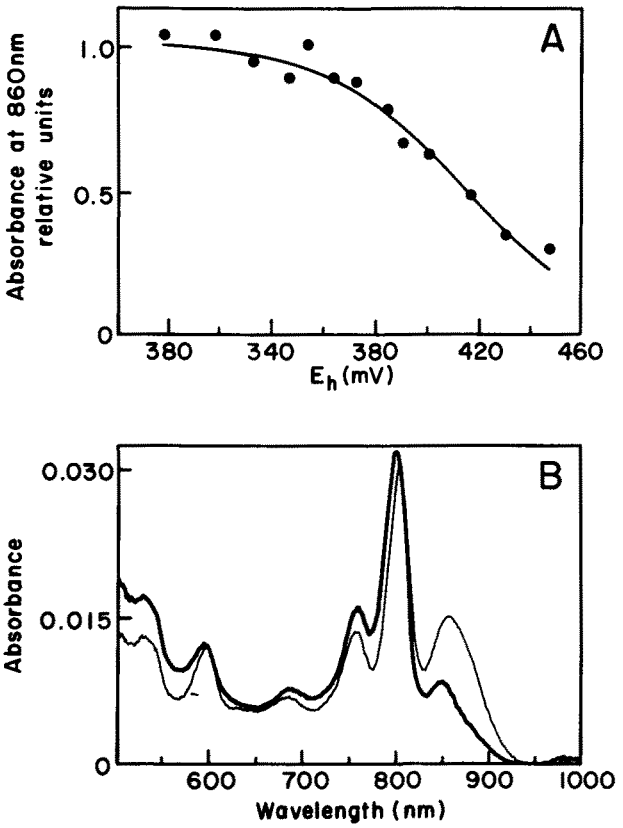

Fig. 10. (A) Redox titration of $BChl_2$ in a six-layer LB film prepared from a 400:1 PL:RC dispersion of *Rb. sphaeroides* performed under the same conditions as in Fig. 9. The vertical axis shows the absorbance at 860 nm normalized at its maximum value at 200 mV. The continuous line is an $n=1$ Nernst fit to the data with $E_{m8}=414$ mV. (B) Absorption spectra of the LB film obtained at 188 mV (———) and at 441 mV (_____).

Fig. 12A shows the corresponding redox titration of

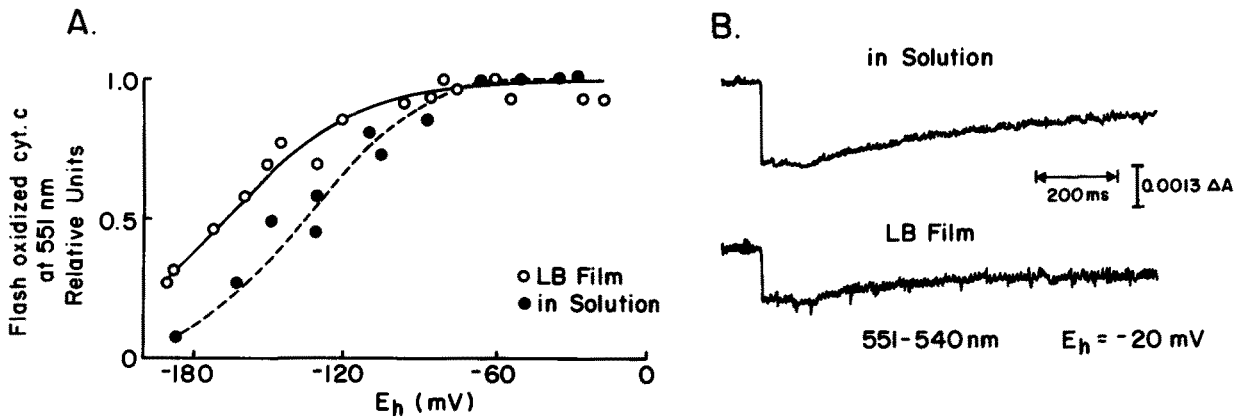

Fig. 11. (A) Redox titration of Q_A in a β:OG dispersion of *Rps. viridis* RC-cyt *c* complex in a 14-layer LB film (○) and in solution (●). The vertical axis represents the absorbance changes associated with cytochrome *c* photo-oxidation at 551 nm following one flash normalized at −20 mV. The slide was placed at 45° to both measuring and excitation beams in a bath containing 60% glycerol, 10 mM Tris-HCl (pH 8.0) and 20 μM each of the following redox mediators: DAD, PMS, PES, TMPD, pyocyanine, phenazine, FeEDTA and DQ. The solid line through the LB film data is an $n=1$ Nernst fit with $E_{m8}=-165$ mV, the dashed line is an analogous fit to the data in solution with $E_{m8}=-130$ mV. (B) Photo-oxidation of the cytochrome *c* complement in both systems measured at 551 nm at a redox potential of −20 mV.

TABLE I

Thermodynamic and kinetic data on the reaction center of Rps. viridis

n.d., not determined.

	LB films		In solution	
	isolated RC	membrane	isolated RC	membrane
E_{m8} $BChl_2$ (mV)	464	n.d.	464	500 [a]
E_{m8} Q_A (mV)	−165	n.d.	−135	−140 [a]
E_{m8} Q_B (mV)	n.d.	n.d.		67 [b]
k $Q_A \rightarrow BChl_2$ (s^{-1})	115	346.5, 27.7 [c]	346 [d]	
k $Q_B \rightarrow BChl_2$ (s^{-1})	4.5	5.4	6.3 [d]	0.017 [d]

[a] From Ref. 29. [b] From Ref. 30. [c] This reaction was observed to be biphasic in the presence of *o*-phen. [d] From Ref. 19.

Q_A^-/Q_A in a multilayer of *Rb. sphaeroides* RCs. The ordinate in this case is the amplitude of the light-induced formation of $BChl_2^+$ measured at 860 nm normalized to its maximum value at an E_h value of 300 mV where, prior to activation, Q_A is fully oxidized. The continuous line is a one-electron fit to the data with an E_{m8} value of −64 mV. In Fig. 12B the absorption transients at E_h values of 195 mV and 0 mV are shown. Fits to these transients indicate 25% fast phase ($k = 9.9$ s^{-1}) and 75% slow phase ($k = 0.77$ s^{-1}) at 195 mV and approx. 99% fast phase at 0 mV. This observation is consistent with the expected inhibition of the Q_A to Q_B electron transfer when Q_B is doubly reduced prior to excitation (the midpoint potential of the couple $Q_B \cdot H/Q_BH_2$ is approx. −40 mV [28], significantly higher than the Q_A^-/Q_A couple). Below 0 mV the kinetics of charge recombination were observed to accelerate by more than 10-fold if the redox bathing solution contained low concentrations of PMS and PES (1–2 μM). Under these conditions the signal disappeared at redox potentials around −50 mV. On the other hand, in the absence of these mediators and relying only on mediation from the lower potential dyes (pyocyanine and phenazine) the kinetics of charge recombination, typical of Q_A^- $BChl_2^+$, remained approximately unchanged from 0 mV down to the redox potential at which no more $BChl_2^+$ could be detected. However, due to the poor redox mediation in the region from 60 mV to −60 mV the data showed some hysteresis. This problem was minimized by allowing longer redox equilibration times (approx. 20 min) in complete darkness.

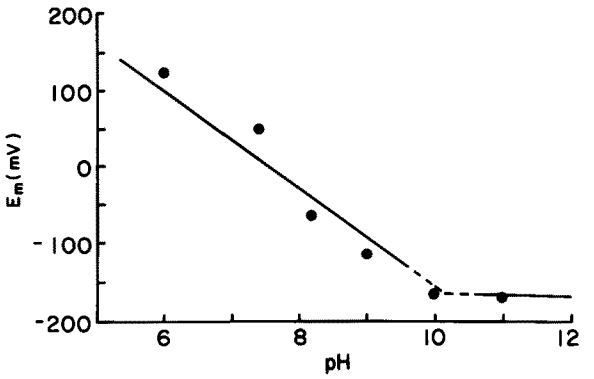

Fig. 13. pH dependence of the midpoint potential of Q_A on a multilayer LB film prepared from a 400:1 PL:RC dispersion of *Rb. sphaeroides* RCs. The midpoints at each potential were determined as in Fig. 12. The pH of the redox bath was adjusted using 10 mM concentrations of: Mes (pH 6), Mops (pH 7), Tris-HCl (pH 8), Ches (pH 9), CAPS (pH 10) and Na_2HPO_4 (pH 11).

The pH dependence of the midpoint potential of Q_A was obtained for the *Rb. sphaeroides* LB films. Fig. 13 shows that the midpoint potential has an approx. −60 mV/pH dependence indicative of a one-electron/one-proton redox couple $Q_A^-(H^+)/Q_A$ with a pK close to 10. Similar properties have been reported for chromatophores in solution; see Discussion. A pH/E_m determination for *Rps. viridis* was not done. Tables I and II summarize the thermodynamic and kinetic characterization of the isolated RC protein films of both species. The values reported in the literature for preparations in solution are also included for comparison.

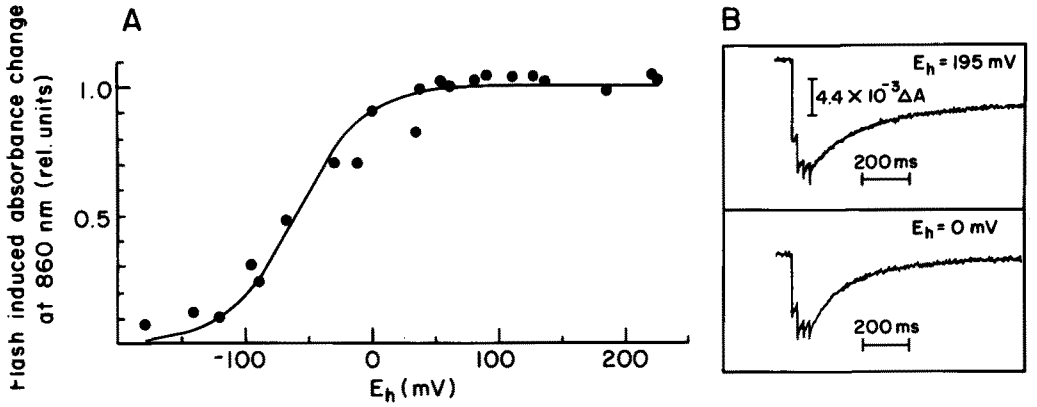

Fig. 12. (A) Redox titration of Q_A in a six-layer LB film prepared from a 400:1 PL:RC dispersion of *Rb. sphaeroides* RCs. The experimental conditions were similar to those in Fig. 11 except that PMS and PES were omitted. The vertical axis shows the absorbance at 860 nm normalized at 300 mV, the continuous line is an $n = 1$ fit to the data with $E_{m8} = -64$ mV. (B) Light-induced absorption transients in the LB film at 860 nm measured at 195 mV (upper trace) and at 0 mV (lower trace).

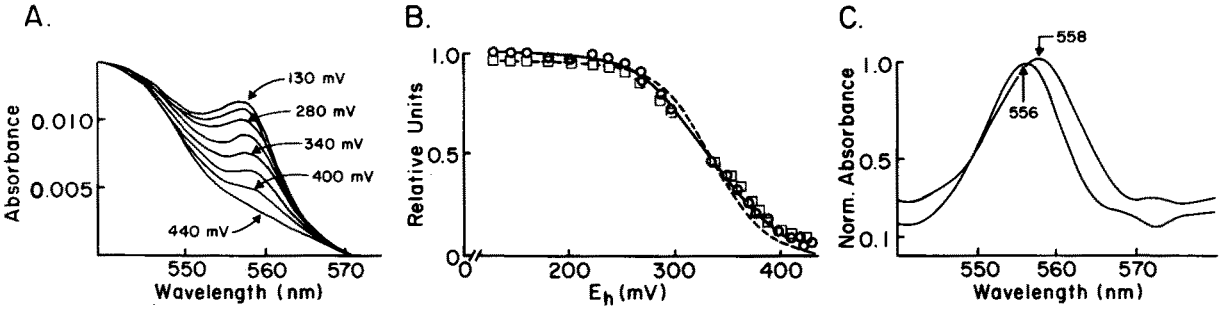

Fig. 14. (A) Cytochrome *c* α-band absorption spectra of a 14-layer LB film prepared from a β:OG dispersion of *Rps. viridis* RC-cyt *c* complex. The slide plane made an angle of 30° to the measuring beam. The redox bath contained 20 mM each of the following mediators: DAD, PMS, PES, pyocyanine, FeEDTA, phenazine and DQ. (B) Redox titration of the differential absorption change at 555 nm relative to a baseline at 440 mV, where the four hemes are 100% oxidized. The amplitude of the absorption at 555 nm was measured at each potential relative to a line connecting the points at 540 and 570 nm in the difference spectra. The signal was normalized at the maximum value attained at 130 mV. The continuous line is a fit to the data with a two component $n=1$ Nernst curve with $E^1_{m8}=370$ mV and $E^2_{m8}=295$ mV. The dashed line shows that a fit with a single $n=1$ Nernst curve ($E_{m8}=330$ mV) systematically deviates from the experimental data. (C) Normalized cytochrome *c* α-band spectra of the two spectral components associated with the two redox centers. The spectrum with the maximum at 558 nm was obtained by a difference spectrum at 370 mV relative to 440 mV while that with a maximum at 556 nm is difference spectrum at 130 mV relative to 295 mV.

(iii) Midpoint potentials of the cytochrome c hemes in the Rps. viridis RC-cyt *c* complex. The redox titrations of the four hemes in the *Rps. viridis* RC-cyt *c* complex as LB films prepared from the three types of dispersion (β-OG, LDAO and PC) were performed in two different ways: (a) One sample was used to titrate all four hemes covering the entire redox range from 440 mV to −180 mV, and (b) with two samples prepared under identical conditions: one of which was used to titrate the high-potential hemes while the other was used for the titration of the low-potential hemes. These steps were taken to check possible damage of the film during the lengthy complete titration (approx. 3 h). The results showed that the two procedures yield essentially the same midpoint potentials, thereby demonstrating the high stability of the deposited films.

Fig. 14A shows difference spectra of a multilayer of *Rps. viridis* RC-cyt *c* complex in β-OG in the E_h range from 440 mV to 130 mV. Fig. 14B illustrates the result of a typical redox titration of the high-potential hemes. The continuous line through the data is a two component, one-electron ($n=1$) Nernst curve fit with E_{m8} values at 370 mV and 295 mV, indicating that the two high-potential hemes represent two electrochemically distinct centers. Fig. 14C shows the spectrophotometric resolution of the two high-potential hemes. The spectra show that the heme with an E_{m8} value of 370 mV has an α-band maximum at 558 nm while that of the heme with an E_{m8} value of 295 mV is at 556 nm.

Fig. 15 shows the redox and absorption properties of the low-potential hemes in a β-OG:RC-cyt *c* multilayer film. Panel B describes a typical titration of the low-potential hemes as determined by measuring the absorption at 551 nm. As in the case of the high-potential hemes, the data were fitted with two, one-electron Nernst curves with E_{m8} values at 50 mV and −51 mV.

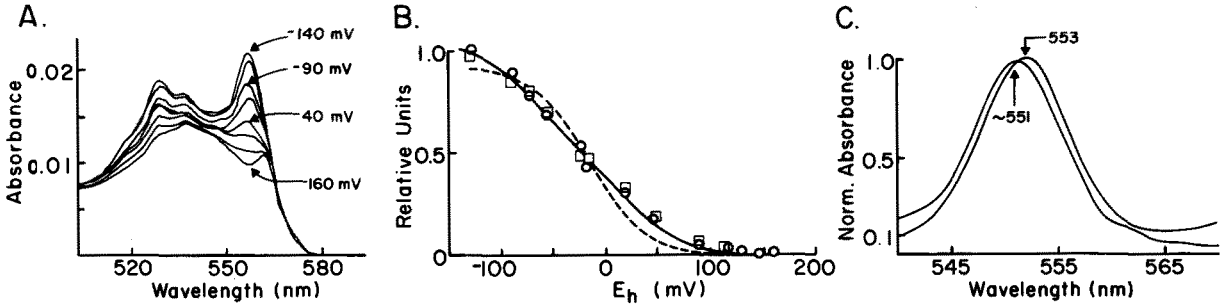

Fig. 15. (A) Cytochrome *c* α-band absorption spectra in the region $-140\text{ mV} \le E_h \le 160$ mV. This is the same film as described in Fig. 14 and the conditions for the titration are the same. (B) Differential absorption at 551 nm relative to that at 130 mV plotted as a function of the redox potential. The amplitude of the absorption was measured relative to a line connecting the points at 503 and 570 nm and was normalized relative to its value at −140 mV. The continuous line is a two component $n=1$ Nernst fit to the data ($E^1_{m8}=50$ mV and $E^2_{m8}=-51$ mV). The dashed line shows the poor quality of a fit to the data with a single $n=1$ Nernst curve ($E_{m8}=-20$ mV). (C) Normalized cytochrome *c* α-band spectra of the two components associated with the resolved redox centers. The spectrum with maximum at 553 nm was obtained by a difference between spectra at −80 mV and 4 mV, while that with a maximum at 551 nm is a difference between spectra at 30 mV and 100 mV.

TABLE II

Thermodynamic and kinetic data on the reaction center of Rb. sphaeroides

	LB films		In solution	
	isolated RC	membrane	isolated RC	membrane
E_{m8} $BChl_2$ (mV)	414	n.d.	440 [a]	440 [b]
E_{m8} Q_A (mV)	−64	n.d.	−45 [c]	−80 [d]
E_{m8} Q_B (mV)	n.d.	n.d.	22 [e]	40 [f]
k $Q_A \rightarrow BChl_2$ (s^{-1})	9.9	n.d.	7 [g]	7 [g]
k $Q_B \rightarrow BChl_2$ (s^{-1})	0.77	n.d.	0.7 [g]	

[a] From Ref. 27. [b] From Ref. 31. [c] From Ref. 32. [d] From Ref. 33. [e] From Ref. 34. [f] From Ref. 27. [g] From Ref. 25.

The spectrophotometric resolution of the two low-potential hemes (Fig. 15C) reveals that the heme with an E_{m8} value of 50 mV has an α-band maximum at 551 nm, while that of the heme with an E_{m8} value of −51 mV is at 553 nm.

Our preliminary observation [5] that the midpoint potentials of the hemes in the deposited films may depend on the type of detergent used to solubilize the RC-cyt *c* complex prompted us to perform more systematic titrations of LB films of RC-cyt *c* complex prepared from dispersions in LDAO, β-OG and phospholipids. The experimental details and quality of the titrations are essentially the same as the ones shown in Figs. 14 and 15. Although the results were in good agreement with those of the β-OG : RC, reproducible variations were found between different types of preparation. Table III summarizes the heme midpoints in the LB films along with other published values (see Discussion).

(d) Light-induced oxidation of the four cytochrome c hemes in a deposited film

With the electrochemical and spectroscopic resolution of the four hemes at hand it becomes feasible to test whether they retain their capability of electron donation to $BChl_2^+$ in the deposited films. This was done by measuring the flash activated cytochrome *c* oxidation under E_h conditions in which one, two, three and all four cytochromes are reduced before activation. The conditions for this are illustrated in Table IV; at each successive lower redox potential an additional heme becomes at least 80% reduced before excitation and hence each of them can readily be tested as a potential electron donor to the photo-oxidized $BChl_2$. Fig. 16 shows the flash-generated oxidized minus reduced α-band spectra of the cytochromes in a multilayer film of RC-cyt *c* complex in β-OG poised at the indicated redox potentials.

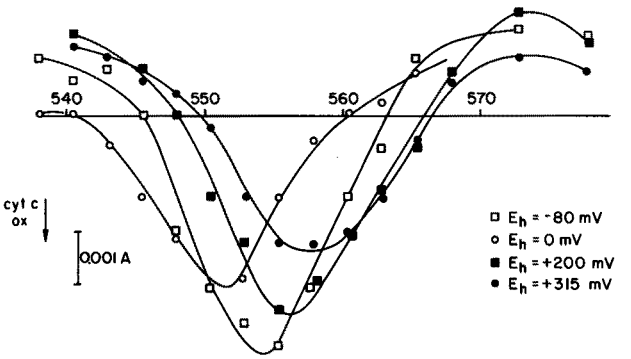

Fig. 16. Spectra of the photo-oxidation of the four hemes in a 14-layer LB film prepared from a dispersion of β : OG RC-cyt *c* complex from *Rps. viridis*. The redox bath composition was as in Figs. 14 and 15. The absorbance changes after a single flash were plotted as a function of the wavelength. The E_h values were chosen to guarantee that at each redox potential change only one extra heme is added in the reduced form and is therefore a donor to the light generated $BChl_2^+$ (see Table IV).

From Fig. 16 it is clear that at each potential the α-band of the stably oxidized cytochrome corresponds with that of the lowest midpoint potential heme of the ones reduced before excitation. This result implies that all four hemes are capable of undergoing oxidation following the generation of $BChl_2^+$. Moreover, we can estimate the halftime of all the oxidation events to be < 50 μs (limit placed by the resolution of our measurements) regardless of the position of the heme in the structure. In the likely event that some of these reactions are not a *direct* electron transfer to $BChl_2^+$, then fast inter heme electron transfers are expected to be involved. At present time there is clear evidence that electron transfer from heme 556 to heme 558 occurs with a halftime of 3.5 μs after the former is oxidized by

TABLE III

Midpoint potentials (mV) of the hemes in Rps. viridis RC-cyt c complex

Heme	LB films: isolated RC-cyt *c* complex			In solution	
	lipids	β-OG	LDAO	isol. RC-cyt *c* complex in Triton [a]	chromatophores [b]
558 nm	360	370	340	380	400
556 nm	279	295	225	310	320
551 nm	25	50	90	20	20
553 nm	−100	−50	−90	−60	−80

[a] From Ref. 35. [b] From Ref. 37.

TABLE IV

Redox state of the cytochrome c complement of the Rps. viridis reaction center

E_h poise (mV)	*Heme* 558 E_{m8} 370	*Heme* 556 E_{m8} 295	*Heme* 551 E_{m8} 50	Heme 553 E_{m8} −50
315	90% red	70% ox	100% ox	100% ox
200	100% red	100% red	100% ox	100% ox
0	100% red	100% red	100% red	80% ox
−80	100% red	100% red	100% red	100% red

$BChl_2^+$ with a halftime of 0.27 μs [35,36]; thus, if similar rates operate in the LB films we would not expect to detect transient kinetics with the instrumentation we used.

3. *Characterization of the Rps. viridis chromatophore films*

(a) Spectral quality and photo-activity of the LB films

Fig. 17 shows the absorption spectrum of a multilayer film of purified *Rps. viridis* chromatophores and that of a dispersion of the same preparation in solution. To aid comparison the spectra are normalized at 1015 nm. It is clear that, aside from a minor increase in the absorbance at 680 nm in the LB film, the spectral properties of the native system have been retained. We have observed that after approx. 1 h of exposure of the LB film to oxidizing redox potentials ($E_h > 400$ mV) the spectra of the chromatophore films exhibit additional increases in the absorbance at 680 nm, while the intensity of the 1015 nm band decreases. However, from measurements of the photooxidizable cytochrome *c* before and after the spectral changes occur it is clear that the RC-cyt *c* complex remains functionally intact. This appears to reflect alterations in the antenna protein rather than the RC-cyt *c* complex itself.

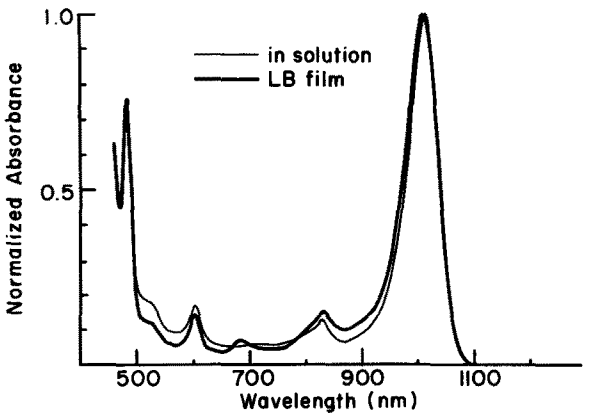

Fig. 17. Absorption spectra of purified *Rps. viridis* chromatophores in a 5-layer LB film (_____) and of the same preparation in solution (———). The LB film spectrum was obtained with the slide at 30° to the measuring beam using non-polarized light. In both cases the medium contained 60% glycerol and 10 mM Tris-HCl (pH 8.0), no redox dyes were used. The spectra were normalized at 1015 nm.

Determination of the RC-cyt *c* complex concentration from the absorption spectrum of the chromatophore LB film is hampered by the spectral overlap with the antenna pigments. However, an estimate of the RC-cyt *c* concentration was obtained from the amount of cytochrome *c* that undergoes flash-induced oxidation when the films are poised at an E_h value of 200 mV with the assumption, based on the work with the isolated RC-cyt *c* complex films, that all the reaction centers are functionally coupled to the cytochrome c. This approach yields a concentration of RC-cyt *c* complex of approx. $2.4 \cdot 10^{12}$ RC/cm^2 per deposition.

Activity assays of the LB films showed that the chromatophore films retained 90–95% of that observed in solution. This compares with maximal activities of 70–80% for isolated RC films and perhaps reflects the more protective environment of the native membrane bilayer. The activity and spectroscopic quality of the films were highly reproducible when the chromatophore preparations satisfied the criteria laid out in Materials and Methods.

(b) Kinetics of electron transfer involving Q_A and Q_B

The kinetics of charge recombination from the states $BChl_2^+Q_A^-$ and $BChl_2^+Q_B^-$ in a chromatophore multilayer were measured by monitoring the light-induced absorption changes at 960 nm. For this purpose the cytochrome *c* complement was oxidized prior to activation by air exposure. It was observed that, upon short time exposure to *o*-phen (15 min), LB films of chromatophores, in contrast to the isolated RC-cyt *c* complex, do not suffer any functional damage; therefore, Q_B functionality was assessed by measuring the kinetics of charge recombination in the absence and presence of *o*-phen. Fig. 18 shows the absorption transients before and after addition of *o*-phen. Curve A was fitted with a two exponential decay with rate constants of 5.4 s^{-1} (85% amplitude) and 231 s^{-1} (15% amplitude). In the presence of approx. 4 mM *o*-phen (curve B) the kinetics appear biphasic with rate constants of 346.5 s^{-1} (88%)

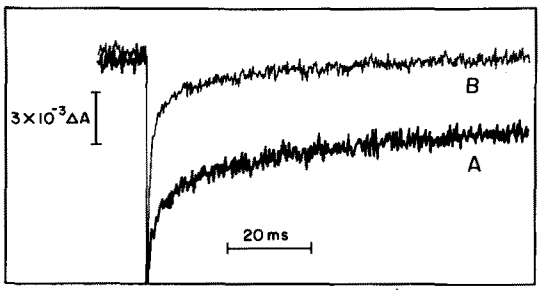

Fig. 18. Light-induced absorption changes at 960 nm associated with the formation of $BChl_2^+$ in a five-layer LB film of purified *Rps. viridis* chromatophores in the absence (A) and presence of 4 mM *o*-phen (B). The transients were measured on a sample in which the hemes were oxidized by exposure of the film to atmospheric oxygen. The reaction medium was as described in Fig. 17.

and 27.7 s^{-1} (12%). These values are in good agreement with those reported for RC-cyt *c* complex in solution [24,38]; these are summarized in Tables I and II.

Analysis of the functionality of the cytochrome *c* complement in the chromatophore LB films was performed as in the isolated RC-cyt *c* complex. As will be shown in the accompanying manuscript [51], the spectroscopic and kinetic properties of the four hemes remained close to those reported for chromatophore membranes in solution.

IV. Discussion

1. Film structure

The surface pressure area measurements that we have described are important indicators of the activity and possible orientation of the photosynthetic apparatus in the LB films when deposited on solid substrates. However, in spite of their diagnostic value, they do not provide any information on the microscopic structure of the films. Nevertheless, preliminary assessments of the film structure can be made by comparing the protein densities in the PC:RC films determined from measurements at the air/water interface with spectroscopic analysis of the deposited film. For instance, in the case of a 400:1 PC:RC film of *Rb. sphaeroides* (Fig. 3B), the film area at a pressure of 25 mN/m is 178 cm^2 for a total number of $7.35 \cdot 10^{16}$ DPPC and $1.84 \cdot 10^{14}$ RC molecules added. From the isotherm for a pure DPPC monolayer in Fig. 3A, the area per molecule of DPPC at a pressure of 25 mN/m is approximately 60 $Å^2$, in good agreement with values reported in the literature [39,40]. Assuming that the DPPC molecules in the DPPC:RC dispersion at the interface form a perfectly packed bilayer such that the polar side of one of the two component monolayers is in touch with the water while the other interacts with the gas phase, the area occupied by $7.35 \cdot 10^{16}$ PC molecules would be 220 cm^2. This is the same as that of a monolayer with half that number of molecules ($7.35 \cdot 10^{16}/2 \times 60$ $Å^2$). On the other hand, assigning a cross-section area of $1.1 \cdot 10^3$ $Å^2$ to the RC [41], a homogeneous distribution of $1.84 \cdot 10^{14}$ molecules with their longitudinal axes spanning the bilayer would contribute approx. 200 cm^2 to the total area. Thus, the area of the 400:1 DPPC:RC dispersion would be approx. 420 cm^2. This number is approx. 2.5-fold larger than the measured area, suggesting that the LB film may contain a fraction of multilamellar domains and or DPPC-RC aggregates. However, due to the uncertainty in the spreading efficiency the discrepancy can in part arise from a fraction of the added material dissolving into the subphase before the compression of the film has started. A similar discrepancy is encountered in similar calculations on DPPC:RC-cyt *c* complexes from *Rps. viridis*.

An analogous assessment of the structure of the chromatophore membrane LB films is obviously complicated by uncertainties in the lipid and protein composition. Our spectroscopic determinations of the concentration of RC-cyt *c* complex in the deposited *Rps. viridis* chromatophore LB films were typically $2 \cdot 10^{12}$ RC/cm^2 with maximal variations of $\pm 50\%$ for different preparations. To the best of our knowledge, no accurate determinations of this parameter are available from structural studies in spite of the quasi-crystalline arrangement of these membranes [42]. Indirect determinations of the density of RCs in the chromatophore membrane of other bacterial species have yielded values of $2.02 \cdot 10^{12}$ RC/cm^2 for *Rb. sphaeroides* strain 2.4.1 [43] and $1.08 \cdot 10^{12}$ RC/cm^2 for the blue-green mutant *Rb. sphaeroides* strain R26 [44], which compare favorably with our results and provide provisional support for the suggestion that in the LB films the bilayer structure of the membrane is retained. However, more direct structural measurements are needed. In this regard, we plan to conduct a detailed structural study of films of both RCs reconstituted in lipids and chromatophore membranes by electron microscopy.

2. Spectral quality

The source of the minor spectral changes for films of isolated RCs of both bacterial species presented in Fig. 4 is not fully understood. As mentioned in the Results section, differences in peak heights reflect preferential absorption due to the orientation of the protein in the film (Fig. 5) and a partially polarized measuring beam However, the shift in the absorption bands are likely to arise from physical changes in the environment around the protein, rather than protein denaturation. Similar changes can be reversibly induced in spectra in solution by increasing the concentration of a variety of detergents (Gunner, M.R. and Dutton, P.L., unpublished observations).

Furthermore, in a study on the effect of hydration on the spectroscopic and functional properties of *Rb. sphaeroides* RCs dried onto glass plates Clayton [45] showed that air drying of the films induced small blue shifts in the major bands of the RC. Further dehydration introduced considerably larger shifts that were accompanied by a substantial (but reversible) loss of activity as seen by a drop in the yield for charge separation. Clayton interpreted the blue shifts accompanying air-drying as arising from higher detergent concentrations as the water content decreased. In the case of our LB films, spectra with the same sample have been taken with the slide in air and dipped in an aqueous solution with no major differences detected (Alegria, G. and Dutton, P.L., unpublished observations). This suggests that unless the inner layers of RCs in the multilayer remain at the same hydration state in

both experimental conditions, differences in hydration from an aqueous medium to that encountered in the laboratory air is not the main source of the spectral changes that we observe.

3. Electrochemistry of the chromophores, kinetics of electron transfer and activity of the LB films

(a) $BChl_2$, Q_A and Q_B

Tables I and II reveal that for both species the E_m values of $BChl_2$ and Q_A in the isolated RC-cyt *c* complex LB films are shifted to more negative values relative to either detergent dispersions of isolated RCs or chromatophores in aqueous solution. However, the midpoint shifts are more significant for LB films of *Rps. viridis*. The spectral shifts observed in the absorption band of $BChl_2$ may be associated with the change in midpoint potential. Table II shows that the midpoint potential of Q_A in *Rb. sphaeroides* in the isolated RC is 40 mV lower compared to that in the chromatophore in solution. Furthermore, very different pH dependencies of the Q_A midpoint have been reported for the two preparations; -60 mV/pH unit in the chromatophore membrane and in RCs incorporated in vesicles [31,32], while no pH dependence in isolated RCs in detergent dispersions over the pH range 5–8 [33]. These observations are still poorly understood; however, the important result as far as the LB films are concerned is that the pH dependence of the Q_A midpoint in the PC : RC LB films is analogous to that in the membrane, indicating that the protonation events coupled to the Q_A oxidation and reduction exhibit similar behavior in the two systems.

It has been demonstrated that in the reaction center of *Rps. viridis* electron transfer from Q_A^- to $BChl_2+$ can be observed to occur predominantly via a thermally activated intermediate involving a relaxed state of BPh^- [24]; see Fig. 1. This accounts for the faster recombination rate at room temperature in this species relative to *Rb. sphaeroides*. Moreover, the magnitude of the energy gap between [BPh Q_A^-] and the thermally achieved [BPh^-Q_A] state has a strong effect on the observed recombination rate. It is therefore possible that the slower kinetics of the reaction Q_A^--$BChl_2^+$ seen in the LB films of *Rps. viridis* are a result of small changes in that energy gap. Furthermore, rapid protolytic reactions coupled to the electron transfer are believed to take place during the thermally active charge recombination (Ref. 38; see also Table I). Since these processes contribute to the apparent ΔG^0 for this reaction, it is conceivable that the changes in the kinetics observed in the LB films may partly reflect alterations in these protonation reactions.

In contrast to the *Rps. viridis* RC-cyt *c* complex, the charge recombination reaction $Q_A^- \cdot BChl_2^+$ in *Rb. sphaeroides* containing the native ubiquinone does not involve a thermally activated route. Instead, it is dominated by the direct process involving a free energy gap of 520 meV. Therefore, small variations in the midpoints of Q_A and $BChl_2$, are not expected to significantly modify this charge recombination process [46]. The minor differences in half-times for this reaction between RCs in solution and in LB films shown in Table II are consistent with this expectation.

Gunner et al. [47] and Woodbury et al. [48] have demonstrated that RCs of *Rb. sphaeroides* can operate using the thermally activated route for charge recombination when the native Q_A is extracted and replaced by quinones with lower midpoint potential. We have observed that the kinetics of charge recombination via the thermal route in anthraquinone substituted RCs from *Rb. sphaeroides* exhibit approx. 5-fold slower rates in LB films as compared to RC dispersions in solution (Alegria, G. and Dutton, P.L., unpublished data). Again, this suggests that, as in the case of *Rps. viridis* LB films, there is an alteration in the energy gap between the [$BPhQ_A^-$] and the thermally activated state [BPh^-Q_A].

Although the midpoint potential for Q_B was not determined in either *Rps. viridis* or *Rb. sphaeroides* LB films, comparable halftimes for charge recombination from $BChl_2^+Q_B^-$ (see Tables I and II) as well as very similar percentage of quinone in the Q_B sites in LB films and in solution suggest that the electrochemistry of Q_B and the Q_A to Q_B electron transfer in the films retain their native properties.

When considering the above spectral, kinetic and electrochemical analysis of the films which demonstrates their robust nature, the problem of the 20–30% activity losses in the RC films appears as a puzzling "all or none" process. However, kinetic alterations in the submicrosecond time-scale leading to loss in yield for the formation of $BChl_2^+Q_A^-$ (see Fig. 1) would not be detected since, the time resolution of our kinetic measurements in this report was approx. 50 μs, and would be consistent with the cryptic character of the loss of activity. Possible sources of such cryptic loss of activity include: loss of Q_A into the subphase, slowing of the electron transfer from BPh^- to Q_A to a point where it approaches the decay of $BChl_2^+BPh^-$ back to the ground state, increase of the decay of $BChl_2^*$ and/or slowing of the electron transfer from $BChl_2^*$ to BPh. In reference to the latter possibility it is worth mentioning that preliminary measurements in the picosecond time-scale indicate that this reaction is unchanged in LB films of *Rb. sphaeroides* (Moser, C.C., Sention, R.S., Dutton, P.L. and Hochstrasser R.M., unpublished results). At this point loss of Q_A would seem the source that is most consistent with the kinetic and thermodynamic data from LB film measurements and RCs in solution. Nevertheless, if this were the case it is difficult to explain why some RCs lose Q_A while others appear to retain both Q_A and Q_B.

(b) Cytochrome c hemes

Table III summarizes the midpoint potentials of the four hemes in the *Rps. viridis* RC-cyt *c* complex obtained with the three types of LB film described in Materials and Methods. For comparison we have also included the midpoints reported by Dracheva et al. [35] in Triton X-100 dispersions of isolated RC-cyt *c* complex and by Nitschke et al. [37] and in chromatophores in solution. As can be seen, the results reported here are in good agreement with those in solution, demonstrating that the hemes in the LB films have retained their in vivo electrochemical properties. However, inspection of Table III reveals that the electrochemical resolution between the two members of each couple in any of the three different types of LB film is enhanced relative to that in isolated RC-cyt *c* complexes in solution. Furthermore, the larger difference in the E_m values between the members of the low-potential couple in the films relative to those in solution points out their higher sensitivity to the nature of their immediate environment. In comparison, the absorption characteristics are less susceptible to environmental variations.

In a recent publication M.R. Gunner and B. Honig [49] successfully reproduced the experimentally determined midpoint potentials of the four hemes in *Rps. viridis*. Their method consisted in the determination of the electrostatic potential throughout the RC-cyt *c* complex by solving the Poisson-Boltzmann equation; they identified the factors that generate the differences in the electrochemistry of the four hemes. In order of importance these were: (a) the presence of acidic and basic residues on the surface of the cytochrome subunit; (b) differences in the stabilization of the charge on the heme by the solvent; (c) the nature of the axial ligands; and (d) interheme interactions. In this context the variations in the electrochemistry of the hemes in the LB films could be ascribed to altered heme solvation; in the environment created in the LB film the hemes are not exposed to a bulk aqueous phase. It has also been shown that the redox properties of heme proteins are very sensitive to the distance between the iron atom and its ligands [50]. From these points of view it is also possible that in the RC-cyt *c* complex LB films these distances have been modified. Regardless of the source(s) of the modified redox properties of the four hemes in the LB films, the results presented in this work show that, within the limits of our experimental resolution, the electron transfer capabilities of the four hemes remained intact.

Acknowledgment

This work was supported by Grant GM 41040–02 from the United States Public Service.

References

1 Moser, C.C. and Dutton, P.L. (1988) Biochemistry 27, 2450–2461.
2 Dracheva, S.M., Drachev, L.A., Zaberezhnaya, S.M., Konstantinov, A.A., Semenov, A.Y. and Skulachev, V.P. (1986) FEBS Lett. 205, 41–46.
3 Dutton, P.L. (1986) Encyclopedia of Plant Physiology, Vol. 19 (Staehelin, L.A. and Antzen, C., eds.), pp. 197–237, Springer, Heidelberg.
4 Tiede, D.M. (1985) Biochim. Biophys. Acta 811, 357–379.
5 Alegria, G and Dutton, P.L. (1987) in Cytochrome Systems (Papa, S., Chance, B. and Ernester, L., eds.), pp. 601–608, Plenum, New York.
6 Alegria, G. and Dutton, P.L. (1988) Biophys. J. 53, 387 (Abstr.).
7 Cohen-Bazire, G., Sistrom, W.R. and Steiner, R.K. (1957) J. Cell Comp. Physiol. 49, 25–68.
8 Jacob, J.S. and Miller, K.R. (1983) Arch. Biochim. Biophys. 223, 282–290.
9 Clayton, R.K. and Wang, R.T. (1971) Methods Enzymol. 23, 696–704.
10 Okamura, M.Y., Steiner, A. and Feher, G. (1974) Biochemistry 13, 1394–1403.
11 Pucheu, N.L., Kerber, N.L. and Garcia, A.F. (1976) Arch. Microbiol. 109, 301–305.
12 Prince, R.C., Tiede, D.M., Thornber, P.J. and Dutton, P.L. (1977) Biochim. Biophys. Acta 462, 467–490.
13 Popovic, Z.D., Kovacs, G.J., Vincett, P.S., Alegria, G. and Dutton, P.L. (1986) Chem. Phys. 110, 227–237.
14 Popovic, Z.D., Kovacs, G.J., Vincett, P.S., Alegria, G. and Dutton, P.L. (1986) Biochim. Biophys. Acta 851, 38–48. :.
15 Trurnit, H.J. (1960) J. Colloid Interface Sci. 15, 1–13.
16 Dutton, P.L. (1978) Methods Enzymol. 54, 411–435.
17 Straley, S.C., Parson, W.W., Mauzerall, D.C. and Clayton, R.K. (1973) Biochim. Biophys. Acta 305, 597–609.
18 Clayton, R.K. and Clayton, B.J. (1978) Biochim. Biophys. Acta 501, 478–487.
19 Shopes,R.J. and Wraight, C.A. (1985) Biochim. Biophys. Acta 806, 348–356.
20 Albrecht, O., Gruler, H. and Sackmann E. (1981) J. Colloid. Interface Sci. 79, 319–339.
21 Heckl, W.M., Losche, M. and Mohwald, H. (1985) Thin Solid Films 133, 73–81.
22 Heckl, W.M., Losche, M, Sheer, H. and Mohwald, H. (1985) Biochim. Biophys. Acta 810, 73–83.
23 Shopes, R.J. and Wraight, C.A. (1986) Biochim. Biophys. Acta 848, 364–371.
24 Shopes, R.J. and Wraight, C.A. (1987) Biochim. Biophys. Acta 893, 409–425.
25 Clayton, R.K. and Yan, H.F. (1972) Biophys. J. 12, 867–881.
26 Trosper, T.L., Benson, D.L. and Thornber, J.P. (1977) Biochim. Biophys. Acta 460, 316–330.
27 Feher, G. and Okamura, M.Y. (1978) in The Photosynthetic Bacteria (Clayton, R.K. and Sistrom, W.R., eds.), pp. 349–386, Plenum, New York.
28 Rutherford, A.W. and Evans, M.C.W. (1980) FEBS Lett. 110, 257–261.
29 Prince, R.C., Leigh, J.S. and Dutton, P.L. (1976) Biochim. Biophys. Acta 440, 622–636.
30 Rutherford, A.W. and Evans, M.C.W. (1979) FEBS Left. 104, 227–230.
31 Dutton, P.L. and Jackson, J.B. (1972) Eur. J. Biochem. 30, 495–510.
32 Wraight, C.A. (1981) Isr. J. Chem. 21, 348–354.
33 Dutton, P.L., Leigh, J.S. and Wraight, C.A. (1973) FEBS Lett. 36, 169–173.
34 Kleinfeld, D., Okamura, M.Y. and Feher, G. (1984) Biochim. Biophys. Acta 766, 126–140.

35 Dracheva, S.M., Drachev, L.A., Konstantinov, A.A., Semenov, A.Y. and Skulachev, V.P. (1988) Eur. J. Biochim. 171, 253–264.
36 Shopes, R.J., Levine, L.M.A., Holten, D. and Wraight, C.A. (1987) Photosynth. Res. 12, 165–180.
37 Nitschke, W. and Rutherford, A.W. (1989) Biochemistry 28, 3161–3167.
38 Sebban, P. and Wraight, C.A. (1989) Biochim. Biophys. Acta 974, 54–65.
39 Phillips, M.C. (1972) Prog. Surf. Membr. Sci. 5, 139–221.
40 Albrecht, O., Gruler, H. and Sackmann, E. (1978) J. Phys. (Paris) 39, 301–313.
41 Yeates, T.O., Komiya, H., Rees, D.C., Allen, J.P. and Feher, G. (1987) Proc. Natl. Acad. Sci. USA 84, 6438–6442.
42 Miller, K.R. (1979) Proc. Natl. Acad. Sci. USA 76, 6415–6419.
43 Packham, N.K., Berriman, J.A. and Jackson, J.B. (1978) FEBS Left. 89, 205–210.
44 Kaplan, S. and Antzen, C.J. (1982) Photosynthesis, Vol. 1, Energy Conversion by Plants and Bacteria (Govindgee, ed.), pp. 65–151, Academic Press, New York.
45 Clayton, R.K. (1978) Biochim. Biophys. Acta 504, 255–264.
46 Gunner, M.R. and Dutton, P.L. (1989) J. Am. Chem. Soc. 111, 3400–3412.
47 Gunner, M.R., Tiede, D.M., Prince, R.C. and Dutton P.L., (1982) in Function of Quinones in Energy Conserving Systems (Trumpower, B.L., ed.), pp. 265–269, Academic Press, New York.
48 Woodbury, N.W.T., Parson, W.W., Gunner, M.R., Prince, R.C. and Dutton, P.L. (1986) Biochim. Biophys. Acta 851, 6–22.
49 Gunner, M.R. and Honig, B. (1990) in Perspectives in Photosynthesis (Jortner, J. and Pullman, B., eds.), pp. 53–60, Kluwer, Dordrecht.
50 Senn, H. and Wuthrich, K. (1985) Q. Rev. Biophys. 18 (2) 111–134.
51 Alegria, G. and Dutton, P.L. (1991) Biochim. Biophys. Acta 1057, 258–272.